NMR Analysis of Enzyme-Catalyzed and Free-Equilibrium Mutarotation Kinetics of Monosaccharides

ARTICLE *in* JOURNAL OF THE AMERICAN CHEMICAL SOCIETY · SEPTEMBER 2004

Impact Factor: 12.11 · DOI: 10.1021/ja047911j · Source: PubMed

4 AUTHORS, INCLUDING:

Kyoung-Seok Ryu
Korea Basic Science Institute KBSI
52 PUBLICATIONS **497** CITATIONS
SEE PROFILE

Changhoon Kim
Macrogen, Seoul, South Korea
17 PUBLICATIONS **188** CITATIONS
SEE PROFILE

Chankyu Park
Konkuk University
107 PUBLICATIONS **1,566** CITATIONS
SEE PROFILE

J|A|C|S
COMMUNICATIONS

Published on Web 07/10/2004

NMR Analysis of Enzyme-Catalyzed and Free-Equilibrium Mutarotation Kinetics of Monosaccharides

Kyoung-Seok Ryu,[†] Changhoon Kim,[‡] Chankyu Park,[‡] and Byong-Seok Choi*,[†]

Yusong-Gu, Gusong-Dong 373-1, Department of Chemistry and National Creative Research Institute Center, Korea Advanced Institute of Science and Technology, Daejon 305-701, South Korea, and Yusong-Gu, Gusong-Dong 373-1, Department of Biological Science, Korea Advanced Institute of Science and Technology, Daejon 305-701, Korea

Received April 12, 2004; E-mail: byongseok.choi@kaist.ac.kr

Monosaccharides typically exist as a cyclical pair of isomers (the α- and *β*-anomers) that differ only in the configuration of the anomeric carbon atom. The spontaneous α-to-*β* conversion (mutarotation) of a pyranose (six-membered) ring is too slow (0.015 min^{-1} for glucose)[1] to support fast-energy generation by an organism if the appropriate metabolic enzyme prefers to use a specific anomer as a substrate. Enzyme-catalyzed α-to-*β* conversions are carried out by mutarotases. Because sugar metabolism such as glycolysis and glycosylation retains the α-to-*β* anomeric specificity, the mutarotase activity is critical for biological processes. The only known mutarotase class is galactose mutarotase (GalM in *Escherichia coli*), which catalyzes the anomeric conversion of both D-glucose and D-galactose. The reason that no other mutarotases have been identified may be due to the lack of a suitable method by which to detect mutarotation that occurs when two anomeric forms are in equilibrium. The conventional method for measuring mutarotation detects a change in optical rotation of a molecule and requires a pure preparation of either the α- or *β*-anomer.[2]

To address the need for a method that measures mutarotation in an equilibrated population of α- and *β*-anomers, we exploited the saturation difference (SD) NMR technique, which could label a specific anomer at equilibrium. This technique works well for examining changes in the configurations of protons that decorate the anomeric carbons of sugars, because the chemical shifts of these protons (the so-called H1′-peaks) are generally well separated from those of other protons. The key feature of SD analysis is the ability to obtain a difference spectrum, in which the first and second free induction decays (FIDs) are obtained by presaturating the selected peak (the H1′ peak of the α- or *β*-anomer) in the first FID and the 0.12 ppm neighborhood of the peak in the second FID (to reduce the minor effect of secondary saturation transfer through the saturated protein) with a 180° shift of the receiver phase. Thus, it is possible to label the saturated peak as an observable substrate, and the equivalent peaks of other anomers are shown only when the fast α-to-*β* conversion is in progress. The intensity of the saturated peak can be used as a concentration reference standard. We previously identified several new mutarotases,[3] one of which is the *Escherica coli* FucU protein, which catalyzes the α-to-*β* conversion of L-fucose and an unusual spontaneous anomeric exchanges of D-ribose (Figure 1). In this report, we analyzed the K_M and k_{cat} for this fucose mutratorase and the exchange rates among four ribose anomers using SD and *T1*-relaxation experiments.

L-fucose mainly exists as the α- and *β*-pyran forms in solution with trace amounts of the furan forms. We designated the saturated and unsaturated pyran peaks as ***A*** and ***B***, respectively (Figure 1A). The saturation transferred peak, which is part of ***B***, is referred as

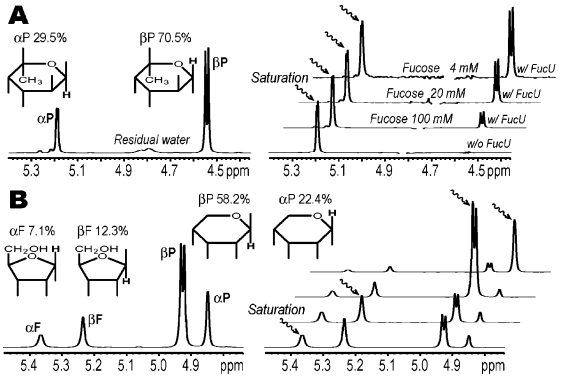

Figure 1. (A) 1D reference spectrum (left) and saturation difference analysis (right) of L-fucose in the presence of FucU (25 *μ*M) at 20 °C. The *β*-pyran peak originated from conversion of the saturated α-pyran via the mutarotase (FucU). The peak ratio of *β*-pyran to saturated α-pyran decreased with increasing concentrations of L-fucose. (B) 1D reference spectrum (left) and saturation difference analysis (right) of D-ribose at 40 °C.

P. For analyzing enzymatic constants ($K_M^{\boldsymbol{A}} = [\boldsymbol{E}][\boldsymbol{A}]/[\boldsymbol{EA}]$ and $V_{max}^{\boldsymbol{A}} = k_2^{\boldsymbol{A}}[\boldsymbol{E}]_T$), the conversion rate ($k_2^{\boldsymbol{A}}\cdot[\boldsymbol{EA}]$) from ***A*** to ***B*** mediated by a mutarotase (***E***) can be simplified in terms of K_M, V_{max}, and the concentration of substrate (***A***) (eq 3) from the Haldane relation at equilibrium ($k_2^{\boldsymbol{A}}\cdot[\boldsymbol{EA}] = k_2^{\boldsymbol{B}}\cdot[\boldsymbol{EB}]$):

$$[E] + [A] \overset{K_A}{\longleftrightarrow} [EA] \overset{k_2^A}{\longrightarrow} [E] + [P] \tag{1}$$

$$[E]_T = [E] + [EA] + [EA]\frac{k_2^A}{k_2^B}, \quad [E]_T = [EA]\cdot\left(\frac{K_M^A}{[A]} + 1 + \frac{k_2^A}{k_2^B}\right) \tag{2}$$

$$\frac{1}{k_2^A[EA]} = \frac{K_M^A}{V_{\max}^A}\cdot\frac{1}{[A]} + \left(\frac{1}{V_{\max}^A} + \frac{1}{V_{\max}^B}\right) \tag{3}$$

After prolonged saturation of ***A*** in the SD experiment, the concentration of ***P*** ($[\boldsymbol{B}]\cdot\boldsymbol{F_P}$, $\boldsymbol{F_P} = [\boldsymbol{P}]/[\boldsymbol{B}]$) is maintained at a certain level through the balance between the increasing (forward conversion, ***A*** to ***P***) and the decreasing pathways (reverse conversion, ***P*** to ***A*** and *T1*-relaxation decay, ***P*** to ***B***). The minor contribution of ***EP*** to the *T1* decay could be negligible $[([\boldsymbol{P}]+[\boldsymbol{EP}])\cdot k_{T1}\cdot[\boldsymbol{P}]\cdot k_{T1}]$, because the amount of ***EP*** is tiny compared with that of ***P***. The Haldane relation also simplifies the forward conversion rate:

$$k_2^A[EA] = k_{T1}[B]F_P + k_2^B[EB]F_P, \quad k_2^A[EA] = \frac{k_{T1}[B]F_p}{1 - F_P} \tag{4}$$

The SD and *T1*-relaxation experiments that are carried out as the concentration of L-fucose increases produce the plot of $1/k_2^{\boldsymbol{A}}[\boldsymbol{EA}]$ *vs* $1/[\boldsymbol{A}]$, in which the slope is equivalent to $K_{cat}^{\boldsymbol{A}}/K_{\mathrm{M}}^{\boldsymbol{A}}$ [65133 ± 974, $(M^{-1}\cdot s^{-1})$] and the *y*-intercept is the sum of $1/V_{max}^{\boldsymbol{A}}$ and $1/V_{max}^{\boldsymbol{B}}$ (Figure 2, left). The plot of $1/k_2^{\boldsymbol{A}}[\boldsymbol{EA}]$ *vs* $1/[\boldsymbol{B}]$ also

[†] Department of Chemistry and National Creative Research Institute Center, Korea Advanced Institute of Science and Technology.
[‡] Department of Biological Science, Korea Advanced Institute of Science and Technology.

10.1021/ja047911j CCC: $27.50

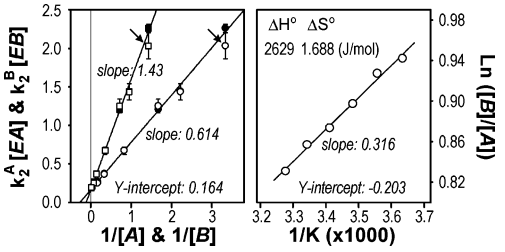

Figure 2. Plot of inverse conversion rate vs inverse concentration of L-fucose (left) and the van't Hoff plot for the ratio of α- and β-anomers (right). The conversion rates obtained from saturation of α-pyran peak (peak A, closed) and β-pyran peak (peak B, open) are the same, because A and B are at equilibrium. The arrow indicates a large deviation from linearity when the concentration of product is low (peak A, 29.5% vs peak B, 70.5%).

provides the K^{B}_{cat}/K^{B}_{M} [27894 ± 417, (M^{-1}·s^{-1})] for the reverse reaction, because the forward and the reverse conversion rates are the same at equilibrium. The plot from the saturation of *B* provides redundant information. Under these conditions, the amount of ***A*** is smaller than that of ***B***, and the reverse conversion rate at low concentrations of L-fucose is more error-prone than the forward rate (marked as an arrow in Figure 2, left). This is because the previous approximation [([***P***] + [***EP***])·k_{T1}·[***P***]·k_{T1}] could not be valid at low amount of ***P*** compared with ***E***. The ideal ratio of V^{A}_{max} and V^{B}_{max} can be determined from their free energy difference, as the Erying transition complexes for the forward and the reverse reactions are the same (principle of microscopic reversibility). In this case, the values of k^{A}_{cat} and k^{B}_{cat} are determined to be 813 ± 18 (s^{-1}) and 348 ± 8 (s^{-1}), respectively, and K^{A}_{M} and K^{B}_{M} have the same value of 12.5 ± 0.27 (mM). Mutarotase should have an identical transition state for the forward and reverse reactions and simply lower the activation energy of reaction, because the different transition states would alter both the V_{max} and K_M to adhere to the Haldane relation. The values K^{A}_{M} and K^{B}_{M} of FucU seem to be the same. In the saturation transfer difference[4] spectrum, the intensities of the methyl protons, which have almost identical T_1-relaxation times (0.764 and 0.784 s for the α- and β-anomer, respectively), are similar to those in the 1D spectrum (see the Supporting Information). These intensities should be the same if the K_M values of FucU for both anomers are the same.

The presence of FucU makes it possible to obtain a van't Hoff plot without the need for a long incubation, because the enzyme accelerates the otherwise slow α-to-β conversion of L-fucoses (Figure 2, right). From the van't Hoff plot, the Δ*H*° and Δ*S*° between two anomers are obtained separately. These results suggest that the difference in the populations of α- and β-anomers ([***A***]/[***B***]) is mainly responsible for the value of Δ*H*°.

Using the same technique, we analyzed the spontaneous nonenzymatic exchange rates of the anomeric equilibria of D-ribose (Figure 1B). D-ribose is the key sugar moiety for the nucleotides, and a considerable amount of the furan form exists in solution compared with that of other monosaccharides, such as D-glucose and L-fucose, which mainly exist as the pyran form. Interestingly, ribose has a higher spontaneous α-to-β exchange rate, even in the pyran forms, compared with that of L-fucose (Figure 1A). Indeed, an extraordinarily high anomeric conversion rate was observed only for the ribofuranoses. However, the exchange rates should correlate with their free energy differences when a simple linear form is assumed to be the intermediate. All exchange rate constants among the four species of D-ribose were determined by analyzing data from SD and *T1*-relaxation experiments (Figure 1B). The saturation time and experimental temperature were increased to 30 s and 40 °C, respectively, for greater accuracy.

Table 1. Exchange Rate Constants (s^{-1})

i→J	A (αF) j	B (βF) j	C (βP) j	D (αP) j
A (αF) i		5.96 e+0 *9.4 e-2	2.09 e-1 *5.6 e-3	1.37 e-1 *5.0 e-3
B (βF) i	3.59 e+0 *5.6 e-2		1.40 e-1 *3.8 e-3	3.17 e-4 *1.1 e-5
C (βP) i	2.65 e-2 *4.2 e-4	4.44 e-2 *7.0 e-4		5.66 e-3 *2.0 e-4
D (αP) i	3.07 e-2 *4.8 e-4	2.43 e-2 *3.8 e-4	1.76 e-2 *4.8 e-4	
T1 (sec)	8.07 e+0 *1.4 e-1	8.09 e+0 *1.4 e-1	7.42 e+0 *4.4 e-1	5.15 e+0 *4.2 e-1

* Errors of rates are derived from the errors of T_1.

Similarly, each exchange process is described by the saturation transfers though the chemical exchanges and its signal decay through *T1*-relaxation. At prolonged saturation of ***A*** (H1′-peak of α-furan), the peaks for $[\boldsymbol{P}]_{\boldsymbol{B}}$ (β-furan), $[\boldsymbol{P}]_{\boldsymbol{C}}$ (β-pyran), and $[\boldsymbol{P}]_{\boldsymbol{D}}$ (α-pyran) are shown through the chemical exchanges not only from the saturated peak ***A***, but also from the secondary exchange processes among the other peaks (***B***, ***C***, and ***D***). $[\boldsymbol{P}]_{\boldsymbol{B}}$ is produced mainly from $[\boldsymbol{S}]_{\boldsymbol{A}}$ (the saturated peak) and secondarily from $[\boldsymbol{P}]_{\boldsymbol{C}}$ and $[\boldsymbol{P}]_{\boldsymbol{D}}$ at the steady state and vanishes through *T1*-relaxation and reverse exchanges into ***A***, ***C***, and ***D*** (eq 5). The concentrations of $[\boldsymbol{P}]_{\boldsymbol{C}}$ (eq 6) and $[\boldsymbol{P}]_{\boldsymbol{D}}$ (eq 7) are expressed in the same way:

$$k_{AB}[S]_A + k_{CB}[P]_C + k_{DB}[P]_D = (k_{BA} + k_{BC} + k_{BD})\cdot[P]_B + k_{T1}[P]_B \quad (5)$$

$$k_{AC}[S]_A + k_{BC}[P]_B + k_{DC}[P]_D = (k_{CA} + k_{CB} + k_{CD})\cdot[P]_C + k_{T1}[P]_C \quad (6)$$

$$k_{AD}[S]_A + k_{BD}[P]_B + k_{CD}[P]_C = (k_{DA} + k_{DB} + k_{DC})\cdot[P]_D + k_{T1}[P]_D \quad (7)$$

We have generated 12 equations (three equations for each of four saturation cases) and have 12 unknown exchange rate constants; thus, the solving of the 12 linear algebraic equations yielded all of the exchange rate constants (Table 1). The most significant feature of Table 1 is that the exchange rate constants for the α- and β-furans are at least one-order of magnitude higher than all of the other rate constants. These results suggest that the intermediates formed during the α-to-β conversion of furans are similar to their original structures, and in contrast, the α-to-β conversion of the pyrans and the furan-to-pyran conversions require more diverse structural rearrangements. The exchange rates did not correlate with the population differences, and the equilibria of D-ribose forms are maintained by the combination of complex exchange processes among the four species. We have also observed fast, spontaneous α-to-β anomeric conversions for D-allose furan forms and ribose 5-phosphate (data not shown). Hence, these findings and the observed high percentage of ribose furan forms could explain the evolutionary selection of ribofuranose, not ribopyranose, as a component of RNA in the RNA world. The specific β-furan form could have been selectively incorporated into RNA during a reaction driven by a stereoselective enzyme or primitive catalyst.

Acknowledgment. This work was supported by the National Creative Research Initiative Program.

Supporting Information Available: Figure of L-fucose methyl protons region of 1D reference and STD spectra which show that K_M of α- and β-anomers for FucU are the same. This material is available free of charge via the Internet at http://pubs.acs.org.

References

(1) Livingstone, G.; Franks, F.; Aspinall, L. J. *J. Solution Chem.* **1977**, *6*, 203−216.
(2) Thoden, J. B.; Kim, J.; Raushel, F. M.; Holden, H. M. *J. Biol. Chem.* **2002**, *277*, 45458−45465.
(3) Ryu, K. S.; Kim, C.; Kim, I.; Yoo, S.; Choi, B. S.; Park, C. *J. Biol. Chem.* **2004**, *279*, 25544−25548.
(4) Mayer, M.; Meyer, B. *J. Am. Chem. Soc.* **2001**, *123*, 6108−6117.

JA047911J